Molecular mechanism of use-dependent calcium channel block by phenylalkylamines: Role of inactivation

(Ca²⁺ channel/phenylalkylamines/state-dependent block/antiarrhythmic action)

Steffen Hering*†, Stefan Aczél*, Richard L. Kraus*, Stanislav Berjukow*, Jörg Striessnig*, and Eugen N. Timin‡

*Institut für Biochemische Pharmakologie, Peter-Mayr-Strasse 1, A-6020 Innsbruck, Austria; and ‡A. V. Vishnevsky Institute of Surgery, 113 039 Moscow, Russia

ABSTRACT The role of channel inactivation in the molecular mechanism of calcium (Ca²⁺) channel block by phenylalkylamines (PAA) was analyzed by designing mutant Ca²⁺ channels that carry the high affinity determinants of the PAA receptor site [Hockerman, G. H., Johnson, B. D., Scheuer, T., and Catterall, W. A. (1995) *J. Biol. Chem.* 270, 22119–22122] but inactivate at different rates. Use-dependent block by PAAs was studied after expressing the mutant Ca²⁺ channels in *Xenopus* oocytes. Substitution of single putative pore-orientated amino acids in segment IIIS6 by alanine (F-1499-A, F-1500-A, F-1510-A, I-1514-A, and F-1515-A) gradually slowed channel inactivation and simultaneously reduced inhibition of barium currents (I_{Ba}) by (−)D600 upon depolarization by 100 ms steps at 0.1 Hz. This apparent reduction in drug sensitivity was only evident if test pulses were applied at a low frequency of 0.1 Hz and almost disappeared at the frequency of 1 Hz. (−)D600 slowed I_{Ba} recovery after maintained membrane depolarization (1–3 sec) to a comparable extent in all channel constructs. A drug-induced delay in the onset of I_{Ba} recovery from inactivation suggests that PAAs promote the transition to a deep inactivated channel conformation. These findings indicate that apparent PAA sensitivity of Ca²⁺ channels is not only defined by drug interaction with its receptor site but also crucially dependent on intrinsic gating properties of the channel molecule. A molecular model for PAA-Ca²⁺ channel interaction that accounts for the relationship between drug induced inactivation and channel block by PAA is proposed.

Voltage gated L-type calcium (Ca²⁺) channels are the therapeutic target for phenylalkylamine (PAA) Ca²⁺ antagonists (1). Channel block by PAA in myocardial (2, 3), smooth muscle (4), and neuronal cells (5) is dependent on the channel conformation (resting, open, inactivated) and accumulates during repetitive depolarization of the membrane. It is widely accepted that this use- (6) or frequency-dependent block plays a significant role in the therapeutic action of PAAs as antiarrhythmics (7). Estimation of use-dependent block of Ca²⁺ channel currents during trains of test pulses serves, therefore, as a classical protocol to study the interaction of PAA with the pore forming α_1 subunit of L-type Ca²⁺ channels. It has been shown that Ca²⁺ channels have to pass through an open conformational state to enable efficient channel block by PAA (3, 4, 8). The role of inactivation in Ca²⁺ channel block by PAA is, however, still not understood. High affinity determinants of the PAA-receptor site of L-type Ca²⁺ channels have recently been identified on transmembrane segment IVS6 by mutating putative pore-orientated amino acids and subsequent screening of the resulting mutants for PAA-sensitivity (8) or by transferring the responsible L-type amino acids into the α_{1A} subunit of P/Q-type channels thereby introducing PAA sensitivity (10, 11). The resulting highly PAA sensitive triple α_{1A} mutant AL25 (11) displayed significantly faster inactivation kinetics than the wild-type channel. Furthermore, an even more rapid inactivation and higher apparent PAA sensitivity was induced into α_{1A} if an additional phenylalanine in position 1,805 of AL25 was mutated to the corresponding L-type methionine in IVS6 suggesting a close link between inactivation properties of the channel and use-dependent block by PAA.

However, because mutations of the PAA-receptor site itself or of closely located amino acids may not only affect channel inactivation but also the interaction of PAAs with their binding site on transmembrane segment IVS6, no unequivocal conclusions about the role of inactivation in channel block could be drawn (11). To answer this question we designed Ca²⁺ channels that inactivate at different rates by site directed mutagenesis of segment IIIS6.

We report here that substitutions of putative pore-lining amino acids that are highly conserved between α_{1A}, α_{1S}, and α_{1C} gradually reduce the rate of channel inactivation while also gradually reducing use-dependent block by (−)D600. Our data indicate that changes in Ca²⁺ channel inactivation induced by site directed mutagenesis modulate use-dependent Ca²⁺ channel block by PAA. This suggests that channel inactivation is an important determinant of use-dependent Ca²⁺ channel block by these drugs.

METHODS

Generation of α_1 Construct. *Chimeric α_1 cDNAs.* Chimeras and mutants were constructed as follows ("silent" restriction sites generated by PCR in previous cloning steps are indicated by asterisks): Chimera AL1 (amino acid composition: α_{1A}1–1406, α_{1S} 965–1104, α_{1A} 1544–1723, α_{1S} 1311–1437, α_{1A} 1856–2424) was as described (12) but with a major portion of the 3′-noncoding region removed. The cDNA of this construct is termed AL1-a. It was constructed by ligating the *Xho*I (nucleotide position α_{1A} 1698)-*Cla*I* (nucleotide position α_{1A} 4925) fragment of the previously published AL1 construct into the respective sites of AL14 (12). Single point mutations were introduced into the *Sal*I* (nucleotide position α_{1S} 3317)-*Cla*I* (nucleotide position α_{1A} 4925) cassette of the AL1-a construct using gene splicing by overlap extension (13). PCR was performed with 35 cycles (1 min at 94°C, 30 sec at 42°C, 1, 5 min at 72°C) using proofreading Pfu polymerase (Stratagene). All

---

PCR-generated mutations were verified by sequence analysis employing the dideoxy chain termination method (14). Single alanine mutations were introduced into the IIIS6 segment at the following positions (amino acid number corresponds to IIIS6 in α_{1A}, (for nomenclature see ref. 15): F1499; F1500, F1510, I1514, and F1515. These residues are located in positions 4, 5, 15, 19, and 20 of IIIS6 from the extracellular side. Therefore the resulting mutants were designated as F4A, F5A, F15A, I19A, F20A, IF19, and 29AA (Fig. 1).

All constructs were inserted into the polyadenylating transcription plasmids pSPCBI-2 (a kind gift of O. Pongs).

Electrophysiology. Inward barium currents (I_{Ba}) were studied with two microelectrode voltage-clamp of *Xenopus* oocytes 2–7 days after microinjection of approximately equimolar cRNA mixtures of α_1 (0.3 ng/50 nl)/β_{1a} (0.1 ng/50 nl)/$\alpha_2\delta$ (0.2 ng/50 nl) as previously described (11, 12). All experiments were carried out at room temperature in a bath solution with the following composition: 40 mM Ba(OH)$_2$, 40 mM *N*-methyl-D-glucamine, 10 mM Hepes, 10 mM glucose (pH adjusted to 7.4 with methanesulfonic acid). Voltage-recording and current-injecting microelectrodes were filled with 2.8 M CsCl, 0.2 M CsOH, 10 mM EGTA, 10 mM Hepes (pH 7.4), and had resistances of 0.3–2 MΩ.

To study the mechanism of Ca^{2+}-channel block by the PAA ($-$)D600 we applied three different pulse protocols: (*i*) measurements of use-dependent I_{Ba} block by PAA during depolarizing pulse trains at different frequencies, (*ii*) estimation of the time course of I_{Ba} recovery from use-dependent block by ($-$)D600, and (*iii*) estimation of I_{Ba} recovery from inactivation and block after a single maintained depolarization.

Use-dependent Ca^{2+} channel block by ($-$)D600 was measured during 15 consecutive 100-ms pulses applied at a frequency of 0.1 Hz or 1 Hz after a 3-min equilibrium period in drug-containing solution at -80 mV. The same pulse trains

were applied in the absence of drug to estimate the accumulation of Ca^{2+} channels in an inactivated state under control conditions. Resting-state dependent block of I_{Ba} (measured as peak current inhibition during the first pulse after a 3-min equilibration in drug containing solution) usually amounted to <10% (see also ref. 11). The holding potential was -80 mV and test potentials were applied to 10 mV that was the peak potential or 10 mV positive to peak of the current-voltage relationships for the channel constructs. The studied point mutations did not affect the current voltage relationship of the resulting mutant channels (data not shown).

Before starting an experiment care was taken to allow the Ca^{2+} channels to recover from inactivation. The oocytes were held for 15–25 min (depending on the batch of oocytes) at -80 mV until I_{Ba} was stable. I_{Ba} of AL1 and the derived mutants were then stable under voltage-clamp conditions for 3–4 hr. For the long recovery experiments this was a clear advantage of class A/L-type chimeras compared with I_{Ba} of chimera Lh that tends to "run down".

Recovery of I_{Ba} from fast inactivation (defined as I_{Ba} recovery within 10 sec) was studied after depolarizing Ca^{2+} channels during a 1 or 3 sec prepulse to 10 mV. The time course of I_{Ba} recovery from inactivation was estimated at a holding potential of -80 mV by applying a test pulse to 10 mV at various time intervals after the conditioning prepulse. Peak I_{Ba} values were normalized to the peak current measured during the prepulse. I_{Ba} recovered between 90–100% during 4 min rest at -100 mV.

I_{Ba} of the chimeric channels decays slowly during maintained depolarization and is described by more than a single exponential. Even a 10 sec pulse to 10 mV did not induce complete inactivation in the channel constructs studied (see Fig. 2*B*). After a 1 sec prepulse (to 10 mV) I_{Ba} recovered within 10 sec to 85–90% of its original value mainly reflecting recovery from the fast component of inactivation. A second slow component of I_{Ba} recovery became prominent if the prepulse length was extended.

Recovery from slow inactivation was measured by applying 10 sec prepulses from -80 to 10 mV and subsequently 20 ms test pulses (to 10 mV) at increasing time intervals starting after a 10 sec interpulse interval to allow the channels to recover from fast inactivation.

I_{Ba}-unblock from use-dependent inhibition by ($-$)D600 was studied at -80 mV by applying a 20 ms test pulse to 10 mV at various time intervals after the last pulse of the train. Because any test pulse applied during the recovery period after a train would induce additional channel block, recovery from use-dependent block was measured only once for a given pulse train. Between subsequent trains and double pulses the membrane voltage was held for 4 min at -100 mV resulting in 90–100% unblock and recovery of the channels from inactivation.
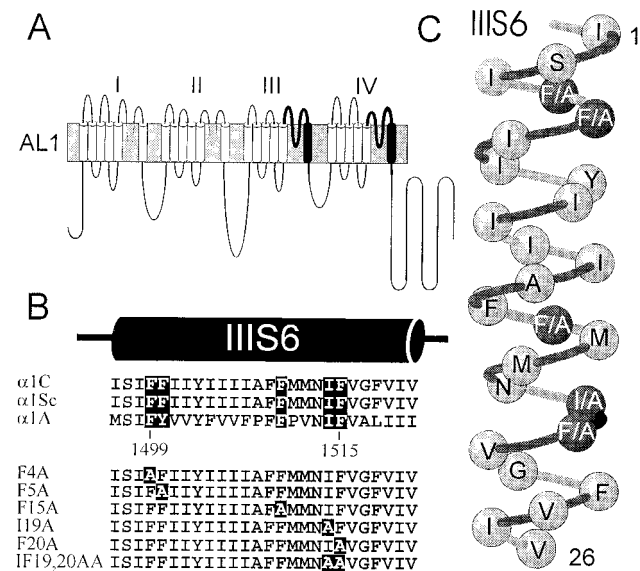

FIG. 1.   (*A*) Schematic representation of chimera AL1 (13) and derived mutants F4A-IF19,20AA. Repeats I and II were from the α_{1A} subunit. L-type sequences that were inserted into the carp skeletal muscle α_{1S} are shown as black transmembrane segments (IIIS6 and IVS6) with bold lines as adjacent S5-S6 connecting loops. (*B*) Sequence alignment (*Lower*) of transmembrane segments IIIS6 of chimera AL1 (the carp skeletal muscle α_{1S}, see 33) and segments IIIS6 of the cardiac L-type α_{1C} (34) and the class A α_{1A} subunit (15). Homologous putative pore-orientated phenylalanines in segment IIIS6 of AL1 and alanine mutations are highlighted. (*C*) Schematic α-helical representation of amino acid sequence of repeat IIIS6 of chimera AL1 (shaded). Substituted putative pore-orientated amino acids of mutants F4A-F20A that are homologous between α_{1A} and α_{1C} are shown (solid).

RESULTS AND DISCUSSION

Putative Pore-Orientated Residues in Segment IIIS6 Affect Ca^{2+} Channel Inactivation and Use-Dependent Ca^{2+} Channel Block by ($-$)D600. We have reported (11) that single amino acid substitutions in transmembrane segments S6 of the α_{1A} subunit affect inactivation of class A Ca^{2+} channels suggesting that S6 segments participate in inactivation gating. To modify Ca^{2+} channel inactivation without affecting the proposed high affinity determinants of PAA interaction within IVS6 we mutated single amino acids in segment IIIS6 of the highly PAA-sensitive class A/L-type chimera AL1 (Fig. 1*A*) (12). Five putative pore-orientated amino acids (four phenylalanines and one isoleucine, see Fig. 1*B*) that are highly conserved in the segments IIIS6 of all known mammalian α_1 subunit isoforms [with exception of F5 (for nomenclature see *Methods*) that is only conserved in L-type Ca^{2+} channels] were substi-
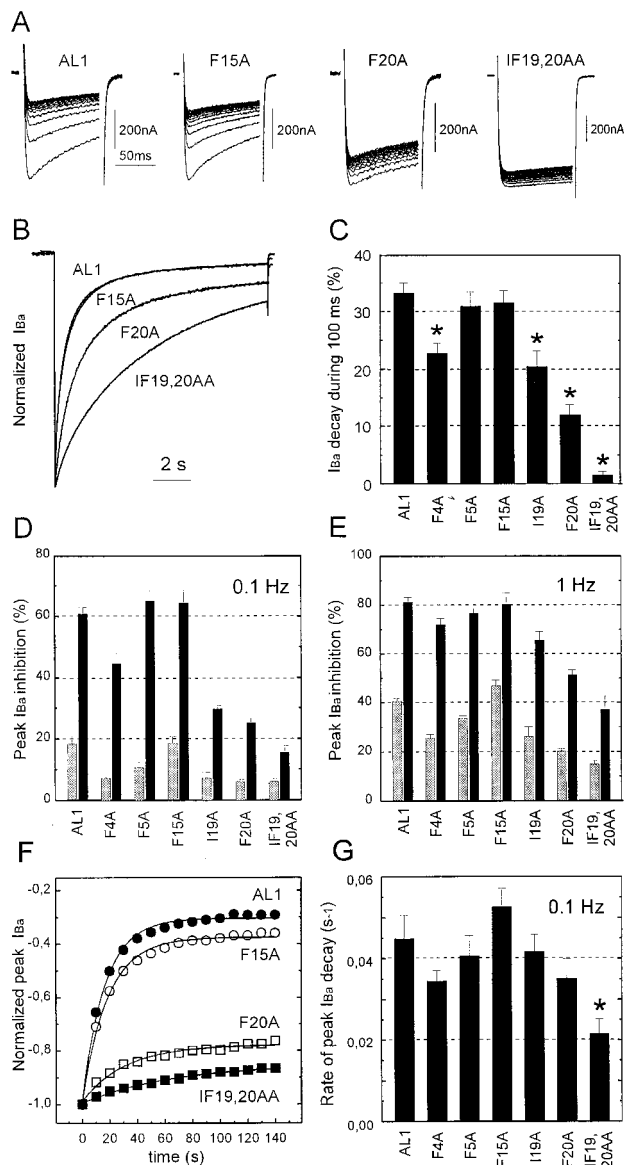
FIG. 2. (*A*) Use-dependent I_{Ba}-inhibition by 100 μM ($-$) gallopamil of AL1, F15A, F20A, and IF19,20AA. Channel block was estimated as peak I_{Ba} inhibition during trains of 15 pulses (100 ms) applied from a holding potential of -80 mV to 10 mV. Note that slowly inactivating mutants are affected less by ($-$)D600! (*B*) Normalized control I_{Ba} of chimeras AL1, F15A, F20A, and IF19,20AA during 10 sec depolarizing test pulses applied from a holding potential of -80 mV to 10 mV. Traces of AL1 and F15A are superimposed. (*C*) Comparison of the time course of I_{Ba} inactivation of mutants AL1, F4A, F5A, F15A, I19A, F20A, and IF19,20AA (in control) measured as I_{Ba}-decay during a 100 ms test pulse from -80 mV to 10 mV ($n = 6$–9). Oocytes were depolarized to the peak potential of the current voltage relationship (10 mV). Statistically significant acceleration of current inactivation compared with AL1 is indicated by asterisks (*$P < 0.05$). (*D* and *E*) Comparison of the use-dependent I_{Ba} block of the AL1 derived mutant α_1 subunits as depicted in Fig. 1 B by 100 μM ($-$)D600. The block of I_{Ba} was measured as cumulative current inhibition (in %) during 15 depolarizing pulses (100 ms) after 3 min incubation of the *Xenopus* oocytes in drug (solid). Peak I_{Ba} decay under control conditions (shaded) indicates an incomplete recovery of I_{Ba} from inactivation during the train. Test pulses were either applied at a frequency of 0.1 Hz (*D*) or 1 Hz (*E*). Bars = mean ± SEM. ($n = 3$–14). (*F*) Peak current values of I_{Ba} in the presence of 100 μM ($-$)D600 during a 0.1 Hz pulse train plotted as a function of time. Smooth lines, single-exponential fits to the time courses with time constants of 16.4 sec (AL1), 18.5 sec (F15A), 31.4 sec (F20A), and 65 sec (IF19,20AA). Data are from the experiments shown in *A*. (*G*) Mean rate constants of peak current inhibition of the studied chimeras

tuted by alanine. Inactivation properties and use-dependent block of the resulting mutants by ($-$)D600 were studied after expression in *Xenopus* oocytes with two microelectrode voltage-clamp.

Alanine substitutions of residues I19 and F20 that are presumably localized closer to the inner mouth of the channel pore, and to an even greater extent the double mutation IF19,20AA (Fig. 1 *B* and *C*) slowed the rate of current inactivation (Fig. 2 *A–C*). Mutation F4A (located presumably closer to the outer channel mouth) also slowed the current inactivation time course and mutants F5A and F15A inactivated with nearly the same rate as AL1 (Fig. 2*B*). Only the reduced rate in current inactivation of I19A, F20A and IF19,20AA was accompanied by a substantial reduction in use-dependent block of I_{Ba} by ($-$)D600 during 100 ms steps at 0.1 Hz. The least amount of block after 15 pulses was observed for chimeras I19A, F20A and the double mutant IF19,20AA whereas chimeras AL1, F4A, F5A, and F15A were strongly blocked by ($-$)D600 during a train (see Fig. 2 *A–D*).

This finding can be explained by mutation-induced alterations in the affinity of the PAA receptor site, changes in channel inactivation properties or both. As the apparent PAA sensitivity was lower in slowly inactivating mutants I19A, F20A, and IF19,20AA compared with faster inactivating AL1, F5A, and F15A it is tempting to speculate that inactivation is an important determinant of PAA block. This was further supported by the finding that an increase in apparent PAA-sensitivity could be induced by depolarizing the membrane at the higher frequency of 1 Hz (Fig. 2*E*). Furthermore, inactivation properties of the chimeras correlated not only with the extent of use-dependent block but also with the rate of block development during a train (Fig. 2 *F* and *G*) suggesting that the rate of I_{Ba} inhibition by ($-$)D600 during a train is substantially determined by the amount of current inactivation during individual pulses.

Evidence for PAA-Induced Inactivation of Ca^{2+} Channels. To enable a more detailed analysis of the role of channel inactivation in block development we studied I_{Ba} block and channel recovery from block after maintained (1 or 3 sec) depolarizations by means of a two-pulse protocol (Fig. 3*A*).

I_{Ba} recovery of our mutant channels from inactivation was estimated at different intervals after a conditioning prepulse at a holding potential of -80 mV (Fig. 3*A*, see *Methods*). Recovery in the absence of drug could be approximated by a single exponential function (Fig. 3 *D* and *E*).

In the presence of ($-$)D600 we consistently observed a small initial delay in the onset of I_{Ba} recovery resulting in a sigmoidal rather than exponential time course. This is illustrated for F15A in Fig. 3 *B* and *C*, where peak I_{Ba} values during a 300-ms recovery interval are shown at a higher time resolution. No significant delay in the onset of I_{Ba} recovery from inactivation was found in the absence of PAA for interpulse intervals down to 20 ms.

An initial delay in I_{Ba} recovery in the presence of ($-$)D600 (in the range of 100 ms) was observed for all our mutant Ca^{2+} channels. This finding was not a peculiarity of our AL1 deduced channel mutants but also observed for the cardiac L-type Ca^{2+} channel construct Lh (12) (see Fig. 3*F* for drug-induced slowing of I_{Ba} recovery from inactivation).

The delay in Ca^{2+} channel recovery in the presence of ($-$)D600 may be explained by recovery of a certain channel fraction from an additional deep or slow inactivated state. Evidence for slow (or ultra slow) inactivation of Ca^{2+} channels

deduced from single exponential fits of the peak I_{Ba} decay during trains of 15 test pulses (100 ms) applied at 0.1 Hz. Peak current values were normalized to the first pulse current amplitude. Statistically significant faster rate of peak current decay during a train compared with AL1 is indicated by * ($P < 0.05$).
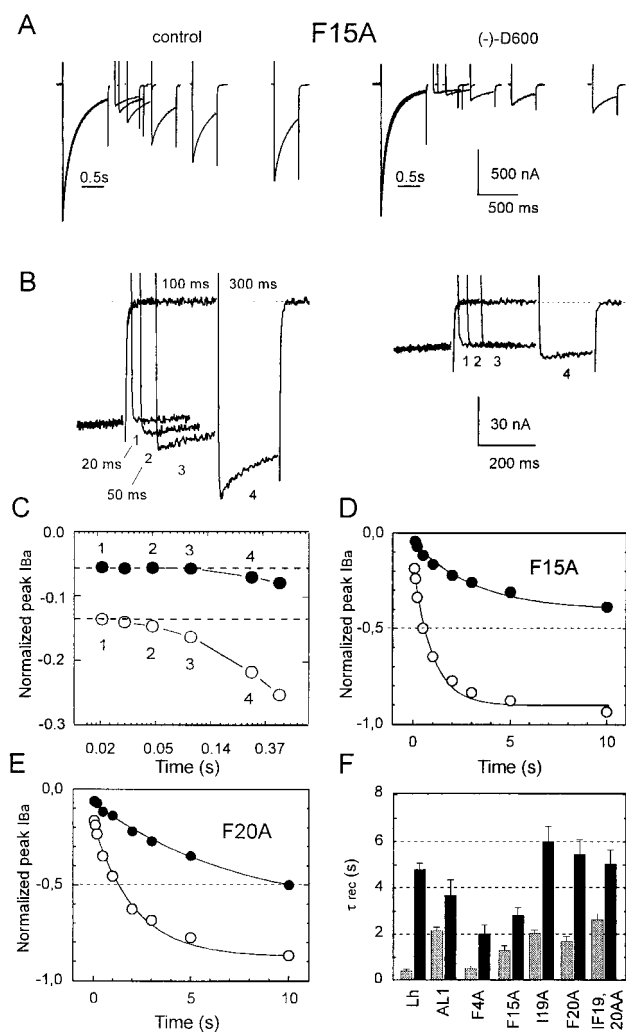
FIG. 3. Delay in recovery of calcium channels in the presence of $(-)$D600. (*A*) I_{Ba} recovery from inactivation of F15A was measured by a two-pulse protocol in the absence (*Left*) and presence of 100 μM $(-)$D600 (*Right*). The currents were inactivated by 1 sec prepulses to 10 mV. Recovery from inactivation at -80 mV was measured by applying a sequence of test pulses at various times (between 50 ms and 10 sec) after the prepulse (see *Methods*). After a two-pulse experiment the membrane was hyperpolarized to -100 mV for 4 min to permit complete recovery from inactivation and block. I_{Ba} measured during the prepulses are superimposed. Mean time constants of recovery from inactivation and block are shown in *F*. (*B*) Initial delay in I_{Ba} recovery from inactivation of F15A in $(-)$D600 (100 μM) at -80 mV after a 1 sec prepulse to 10 mV. Displayed currents were recorded after interpulse intervals of 20, 50, 100, and 300 ms. (*C*) Semilogarithmic plot of peak I_{Ba} during the early phase of recovery (same experiment as shown in *B*). I_{Ba} in the presence of $(-)$D600 recovered with a initial delay of about 100 ms (●). No delay above 20 ms could be observed in the absence of drug(μ). (*D* and *E*) Quantitative analysis of the I_{Ba} recovery from fast inactivation of chimeras Lh (*C*), F15A (*D*), and F20A (*E*). I_{Ba} recovery was measured at -80 mV with the two-pulse protocol as shown in *A*. Peak current values measured at different intervals after the prepulse in control (○) and the presence of 100 μM $(-)$D600 (●) were normalized to peak current values of the prepulse and plotted as a function of time. Data points are fitted by a single exponential function. Continuous lines are single exponential fits to the time courses, with time constants of $\tau_{control} = 0.55$ sec, $\tau_{(-)D600} = 3.85$ sec (Lh, *C*); $\tau_{control} = 0.93$ sec, $\tau_{(-)D600} = 2.76$ sec (F15A, *D*) and $\tau_{control} = 1.86$ sec, $\tau_{(-)D600} = 6.5$ sec (F20A, *E*). (*F*) Mean time constants of I_{Ba} recovery from inactivation in control (shaded) compared with recovery time constants in the presence of 100 μM $(-)$D600 (solid) of chimeras Lh, AL1, F15A, I19A, F20A, and IF19,20AA. Because of the slower time course of inactivation I_{Ba}-recovery of the cardiac construct Lh (12) and IF19,20AA were estimated after 3 sec pulses; recovery of other channel constructs was measured after 1 sec pulses.

was recently presented by Boyett *et al.* (16) who described that a second (slow) phase in recovery of current is enhanced with prolonged membrane depolarization and suggested an important role of slow inactivation for the rate dependent shortening of the action potential in ventricular cells as well as for changes in the conduction velocity of the atrioventricular node.

The most striking result was, however, that $(-)$D600 delayed I_{Ba} recovery of the apparently low-sensitivity F20A and IF19,20AA to a comparable or even higher extent (F20A) as of mutants AL1 and F15A that displayed significantly more use-dependent block during low frequency pulse trains (Fig. 2 *D* and *F*). Thus, after single maintained depolarizations that allow substantial inactivation also in the slowly inactivating I19A, F20A, and IF19,20AA, apparent differences in PAA sensitivity were no longer observed. This clearly indicates that Ca^{2+} channel block by PAA is not only determined by the absolute drug affinity for a specific receptor site but also by the intrinsic gating properties of the channel molecule.

Putative Pore-Orientated Amino Acids in Segment IIIS6 Affect Recovery of Ca^{2+} Channels from Inactivation. Alanine substitutions of putative pore-orientated residues in IIIS6 of chimera AL1 affected not only the rate of I_{Ba} recovery from channel block but also modulated the recovery from inactivation in the absence of drug (Fig. 3*F*).

Compared with I_{Ba} recovery of AL1 ($\tau_{rec./AL1} = 2.13 \pm 0.12$ sec, $n = 3$), chimera F4A, with the alanine substitution located close to the outer mouth of the channel, displayed markedly faster recovery kinetics ($\tau_{rec./F4A} = 0.62 \pm 0.04$ sec, $n = 3$, $P < 0.05$) whereas mutations I19A ($\tau_{rec./I19A} = 2.04 \pm 0.15$ sec, $n = 3$, $P < 0.05$), F20A, and IF19,20FA that are located closer to the inner mouth of the channel pore (Fig. 1*C*) affect I_{Ba} recovery to a lesser extent ($\tau_{rec./F20A} = 1.64 \pm 0.23$ sec, $n = 3$ and $\tau_{rec./IF19,20AA} = 2.58 \pm 0.29$ sec, $n = 3$, not significantly different to AL1) (Fig. 3*F*).

These results reveal that in addition to segment IVS6 (11) and IS6 (17) putative pore-orientated amino acids in transmembrane segment IIIS6 determine kinetics of Ca^{2+} channel inactivation and recovery from inactivation (Fig. 3 and 4) and support our previous hypothesis that pore-lining amino acids of transmembrane segments S6 contribute to Ca^{2+} channel inactivation (11). Our data obtained with chimeric channel constructs should prompt further studies to investigate the role of highly conserved IIIS6 residues F4, F15, I19, and F20 in inactivation gating of the different Ca^{2+} channel types.

Recovery of I_{Ba} from Slow Inactivation and Block by $(-)$D600. If PAAs promote slow inactivation it is likely that recovery from block at rest (-80 mV) occurs with a comparable time course as recovery from a slow inactivated state that is induced by maintained membrane depolarization in the absence of drug. We therefore studied a possible correlation between both processes by investigating I_{Ba} recovery after prolonged (10 sec) depolarizations in two fast inactivating ("high sensitive", AL1 and F15A) and two slowly inactivating ("low sensitive", F20A and IF19,20AA) chimeras in greater detail. Typical time courses of the slow component of I_{Ba} recovery of AL1 are shown in Fig. 4*A*. The mean time constants of I_{Ba} recovery from slow inactivation and the time constant of recovery from use-dependent block by $(-)$D600 of AL1, F15A, F20A and IF19,20AA are compared in Fig. 4*B*. Only I_{Ba} of chimera IF19,20AA recovered significantly faster from block than from slow inactivation in the absence of drug.

Molecular Model for Ca^{2+} Channel Block by PAA. To explain the role of inactivation in use-dependent Ca^{2+} channel block by PAA we propose the model shown in Fig. 4*C*. It is well established (18–23) that PAAs approach their receptor site in the channel pore from the cytoplasmic site. Furthermore, we have recently unequivocally demonstrated in mammalian cells and mutant Ca^{2+} channels expressed in *Xenopus* oocytes that intracellular but not extracellular action of quaternary PAA is strictly use-dependent (24, 25). This finding indicates that
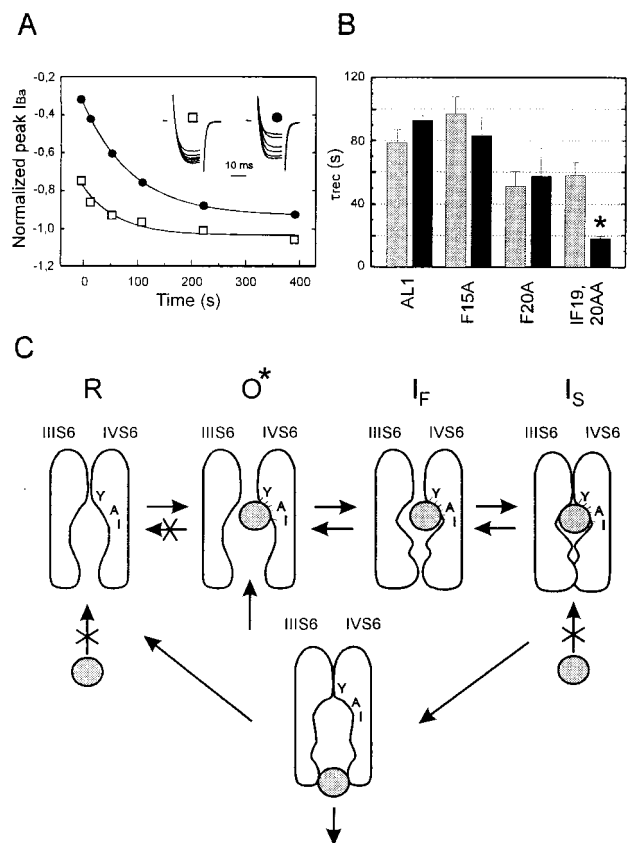
FIG. 4. I_{Ba} recovery from slow inactivation and unblock from use-dependent block by 100 μM ($-$)D600. (*A*) ($\square$) Time course of the slow component in AL1 I_{Ba} recovery from inactivation in control after a 10 sec prepulse to 10 mV (see *Methods*). ($\bullet$) Time course of peak I_{Ba} recovery from block by 100 μM ($-$)D600 induced by 15 test pulses (100 ms) applied at 0.1 Hz pulses from -80 mV to 10 mV in oocytes expressing the fast inactivating chimera AL1. The inset shows I_{Ba} during 20 ms test pulses to 10 mV applied at different intervals after a single 10 sec prepulse to 10 mV ($\square$) or use-dependent block ($\bullet$). Peak current values are normalized (see *Inset*) to I_{Ba} of the prepulse ($\square$) or to the first current of the train ($\bullet$), respectively. Time courses of I_{Ba} recovery from use-dependent block and inactivation were fitted to single exponential functions; respective time constants are $\tau_{unblock}$ = 94 sec and τ_{slow} = 68 sec. (*B*) Mean time constants of I_{Ba} recovery from inactivation (shaded) and from use-dependent block (solid) by 100 μM ($-$)D600 of chimeras AL1, F15A, and F20A. To observe a significant amount of I_{Ba} inhibition during a 0.1 Hz train in IF19,20AA we increased the applied ($-$)D600 concentration to 300 μM. Statistical significant difference in recovery from block and inactivation is indicated by asterisks (*$P < 0.05$). (*C*) Model for PAA interaction with Ca^{2+} channels illustrating drug induced slow inactivation. Access of the PAA molecule (symbolized by the grey ball) to the receptor site in the resting state (R) is restricted. After removal of putative pore-orientated guarding amino acids the drug can enter the channel from the cytoplasmic site in the open conformational state (O*) and subsequently interact with its receptor site (24, 25). According to (8) pore-orientated amino acids of transmembrane segment IVS6 contribute high affinity determinants of the PAA receptor site (11, 25). After PAA interaction with its receptor site the channels become non conducting and transitions of Ca^{2+} channels to the resting state are restricted (see also refs. 27 and 28). If activation and inactivation are coupled processes Ca^{2+} channels will move to the fast inactivated state (I$_F$) and subsequently accumulate in the slow inactivated state (I$_S$) even if the drug does not directly affect the rate of Ca^{2+} channel inactivation. Consequently the amount of use-dependent block during a train of pulses will crucially depend on the rate of channel inactivation (see Fig. 2).

PAAs access the channel via a hydrophilic pathway whereas putative pore-orientated amino acids localized in the cytoplasmic direction from the PAA receptor serve as "guarding"

structures (26) that prevent channel block at rest. Inactivation *per se* is insufficient for channel block by PAA (3, 4) and PAAs therefore access their site upon channel opening after removal of these guarding structures.

The PAA-induced delay in the onset of recovery from inactivation (Fig. 3 *B* and *C*) suggests that after the drug has entered the channel in the open state transitions to I$_S$ occur at a promoted rate (see model in Fig. 4*C*). In our model we offer an explanation for this finding that is deduced from a model earlier described by Armstrong (ref. 27, also ref. 28, see ref. 9 for review), namely that transitions to the resting state are restricted once the drug is bound to the channel in its open conformation. The primary result of the present study that faster inactivating Ca^{2+} channels are more efficiently blocked by PAA can therefore be explained without requiring that PAA directly affect the rate of channel inactivation. Such a model predicts that enhanced accumulation of channels in an inactivated state (observed as use-dependent block by PAA) will occur if Ca^{2+} channels inactivate at a higher rate (AL1, F5A, and F15A) and also explains that slowly inactivating channels (I19A, F20A, IF19,20AA) are blocked more efficiently at a higher frequency of depolarization (Fig. 2 *D* and *E*) or prolonged depolarization by single conditioning pulses (Fig. 3*F*). It has, however, to be emphasized that the indicated changes in channel gating (crossing out of the O $\rightarrow$ R pathway) are the result of a specific PAA-interaction with its binding site. This is supported by our recent finding that accelerated inactivation *per se* does not promote use-dependent PAA-block of class A/L-type chimeric channels lacking the high-affinity determinants in IVS6 (25).

Furthermore, the model provides also an explanation for differences observed for PAA sensitivity in previous studies. Faster inactivating Ca^{2+} currents were found to be more efficiently blocked by PAA than more slowly inactivating Ba^{2+} currents in cardiomyocytes (2). Heterologously expressed L-type Ca^{2+} channels are blocked to a larger extent by PAA when β_3-subunits, which accelerate current inactivation, are coexpressed with α_{1C} (29).

An unexpected finding was, however, that channel PAA-unblock of IF19,20AA occurred at a significantly faster rate than recovery of I_{Ba} from inactivation.

We found that only alanine substitutions close to the cytoplasmic channel mouth affect *both* inactivation and use-dependent I_{Ba} block by PAA. This is illustrated in Figs. 2 and 3 where F4A (close to the outer channel mouth) and I19A (close to the inner channel mouth) inactivate at a comparable rate. However, at low stimulation frequency (0.1 Hz) I19A channels were blocked to a lesser extent than F4A (Fig. 2*D*). It is therefore tempting to speculate, that bulky amino acids I19 and F20 at the inner mouth of the channel in segment IIIS6 (Figs. 1*C* and 4*C*) form part of an inactivation mechanism that prevents drug dissociation from the cytoplasmic side at rest. A single point mutation (I19A or F20A) would weaken its interaction with a putative inactivation particle (Fig. 2 *B* and *C*) but not affect PAA dissociation from its trapped state such that recovery from inactivation remains a rate limiting factor (Fig. 4*B*). Substitution of both residues by alanine removes inactivation to an extent that this process is no longer rate limiting and PAA dissociation at negative voltages occurs at a facilitated rate (Fig. 4*B*). A key role of the I19,F20-motive at the inner channel mouth is also indirectly supported by our recent finding that mutations of the PAA-receptor site itself (i.e., in the central part of the putative IVS6 alpha helix) have no significant effect on the PAA-dissociation rate (25).

In summary our results are consistent with the idea that PAA access a high affinity receptor site in the open channel conformation where I19 and F20 are likely to participate in forming a receptor site for an inactivation structure determining drug dissociation (Fig. 4*C*).

Although our data convincingly demonstrate that inactivation plays a key role in Ca^{2+} channel block by PAA we can, however, not exclude a direct PAA-interaction with I19 and/or F20 in segment IIIS6. We presently favour a model where unblock is substantially determined by removal of inactivation rather than by state independent barrier structures in the pore. Further detailed studies of the voltage dependency of channel unblock are needed for a precise understanding of the molecular pathways of PAA-dissociation from its receptor site in the channel pore. Future research will show if slow inactivation that occurs as a consequence of open channel block by PAA is identical to the ultra slow inactivation of Ca^{2+} channels described under physiological conditions (16).

A delay in recovery from inactivation (Fig. 3 *B* and *C*) was previously observed for sodium channel inactivation and attributed to channel transitions to an additional (slow) inactivated state (30). Accumulation of sodium channels in a slow inactivated state by local anesthetics is induced by long lasting depolarization; channels recover from a slow inactivated state with time constants ranging from several secs to minutes (see ref. 9 for review). By analogy to sodium channel interaction with local anesthetics (9, 31, 32) slow inactivation may consequently have an important role in the antiarrhythmic action of Ca^{2+} antagonists.

1. Catterall, W. A. & Striessnig, J. (1992) *Trends Pharmacol. Sci.* **13,** 256–262.
2. Lee, K. S. & Tsien, R. W. (1983) *Nature (London)* **302,** 790–794.
3. McDonald, T. F., Pelzer, D. & Trautwein, W. (1984) *J. Physiol. (London)* **352,** 217–241.
4. Hering, S., Bolton, T. B., Beech, D. J. & Lim, S. P. (1989) *Circ. Res.* **64,** 928–936.
5. Oyama, Y., Hori, N., Tokutomi, N. & Akaike, N. (1987) *Brain. Res.* **417,** 143–147.
6. Courtney, K. R. (1975) *J. Pharmacol. Exp. Ther.* **195,** 225–236.
7. Hondeghem, L. M. & Katzung, B. G. (1984) *Annu. Rev. Pharacol. Toxicol.* **24,** 387–423.
8. Hockerman, G. H., Johnson, B. D., Scheuer, T. & Catterall, W. A. (1995) *J. Biol. Chem.* **270,** 22119–22122.
9. Hille, B. (1992) *Ionic Channels of Excitable Membranes* (Sinauer, Sunderland, MA).
10. Döring, F., Degtiar, V. E., Grabner, M., Striessnig, J., Hering, S. & Glossmann, H. (1996) *J. Biol. Chem.* **271,** 11745–11749.
11. Hering, S., Aczél, S., Grabner, M., Döring, F., Berjukow, S., Mitterdorfer, J., Sinnegger, M. J., Striessnig, J., Degtiar, D. E., Wang, Z. & Glossmann, H. (1996) *J. Biol. Chem.* **271,** 24471–24475.
12. Grabner, M., Wang, Z., Hering, S., Striessnig, J. & Glossmann, H. (1996) *Neuron* **16,** 207–218.
13. Horton, R. M., Hunt, H. D., Ho. S. N., Pullen, J. K. & Pease, L. R. (1989) *Gene* **77,** 61–68.
14. Sanger, F., Nicklen, S. & Coulson, A. R. (1977) *Proc. Natl. Acad. Sci. USA* **74,** 5463–5467.
15. Mori, Y., Friedrich, T., Kim, M.-S., Mikami, A., Nakai, J., Ruth, P., Bosse, E., Hofmann, F., Flockerzi, V., Furuichi, T., Mikoshiba, K., Imoto, K., Tanabe, T. & Numa, S. (1991) *Nature (London)* **350,** 398–402.
16. Boyett, M, R., Honjo, H., Harrison S. M., Zang W.-J. & Kirby, M. S. (1994) *Pflügers Arch.* **428,** 39–50.
17. Zhang, J.-F., Ellinor, P. T., Aldrich, R. W. & Tsien, R. W. (1994) *Nature (London)* **372,** 97–100.
18. Hescheler, J., Pelzer D., Trube, G. & Trautwein, W. (1982) *Pflügers Arch.* **393,** 287–291.
19. White, E. J. & Bradford, H. F. (1986) *Eur. J. Pharmacol.* **130,** 243–248.
20. Kass, R. S., Arena, J. P. & Chin, S. (1991) *J. Gen. Physiol.* **98,** 63–75.
21. Klöckner, U. & Isenberg, G. (1991) *J. Physiol. Pharmacol.* **42,** 163–179.
22. Hering, S., Savchenko, A., Strübing, C., Lakitsch, M. & Striessnig, J. (1993) *Mol. Pharmacol.* **43,** 820–826.
23. Seydl, K., Kimball, D., Schindler, H. & Romanin, C. (1993) *Pflügers Arch.* **424,** 552–554.
24. Berjukov, S., Aczel, S., Beyer, B., Kimball, D., Dichtl, M., Hering, S. & Striessnig, J. (1996) *Br. J. Pharmacol.* **119,** 1197–1202.
25. Degtiar, V., Aczél, S., Döring, F., Timin, E. N., Kimball, D., Mitterdorfer, J. & Hering, S. (1997) *Biophys. J.* **73,** 157–167.
26. Starmer, C. F. & Grant, A. O. (1985) *Mol. Pharmacol.* **28,** 348–356.
27. Armstrong, C. M. (1971) *J. Gen. Physiol.* **58,** 413–437.
28. Armstrong, C. M. & Bezanilla, F. (1977) *J. Gen. Physiol.* **70,** 567–590.
29. Lacinova, L., Ludwig, A., Bosse, E., Flockerzi, V. & Hofmann, F. (1995) *FEBS Lett.* **373,** 103–107.
30. Chiu, S. Y. (1977) *J. Physiol. (London)* **237,** 573–596.
31. Khodorov, B. I., Shishkova, L. D. & Peganov, E. (1974) *Exp. Biol. Med.* **3,** 10–14.
32. Khodorov, B. I., Shishkova, L. D., Peganov, E. & Revenko, S. (1976) *Biochem. Biophys. Acta* **433,** 409–435.
33. Grabner, M., Friedrich, K., Knaus, H.-G., Striessnig, J., Scheffauer, F., Staudinger, R., Koch, W. J., Schwartz, A. & Glossmann, H. (1991) *Proc. Natl. Acad. Sci. USA* **88,** 727–731.
34. Mikami, A., Imoto, K., Tanabe, T., Niidome, T., Mori, Y., Takeshima, H., Narumiya, S. & Numa, S. (1989) *Nature (London)* **340,** 230–233.